molecular pharmaceutics

articles

Effects of Metal Ions on Entero-Soluble Poly(methacrylic acid-methyl methacrylate) Coating: A Combined Analysis by ATR-FTIR Spectroscopy and Computational Approaches

Francesco Cilurzo, Chiara G. M. Gennari, Francesca Selmin, and Giulio Vistoli*

Department of Pharmaceutical Sciences "Pietro Pratesi", Università degli Studi di Milano, via L. Mangiagalli, 25, 20133 Milan, Italy

Received August 12, 2009; Revised Manuscript Received November 26, 2009; Accepted January 6, 2010

Abstract: Poly(methacrylic acid-methyl methacrylate)s (HPMMs) are pH-dependent polymers which ionize and form salts (PMMs) in neutral conditions. Despite their wide use in tablet coating, the interactions of PMMs with electrolytes present in biorelevant media and luminal fluids have been scantly investigated. The data generated in the current work provide the basic information on the effect of bivalent cations, namely, Ca^{2+}, Zn^{2+} and Mn^{2+}, on the HPMMs' solubility and, consequently, on the performances (disintegration and drug dissolution) of acetaminophen gastroresistant tablets when exposed to fluid containing such salts. The interactions between polymers and metal ions were analyzed by ATR-FTIR spectroscopy and in silico combining molecular dynamics simulations to explore the conformational profiles of several oligomers with different M_w, taken as model of the polymers, with ab initio and semiempirical calculations in the gas phase. The computational results agree with the experimental data in terms of spatial disposition of the bications with respect to PMMs (Ca^{2+} and Mn^{2+} as bidentate form and Zn^{2+} as monodentate ligand) and interaction strength ($Zn^{2+} > Mn^{2+} > Ca^{2+}$). The tablet disintegration and dissolution rate of acetaminophen were strongly affected by the interactions of the dissolving copolymer with the metal ions which led to coating insolubilization. These preliminary results underline that the ingestion of metal ions at high concentrations could affect the drug liberation from gastroresistant dosage forms.

Keywords: Modeling; pH responsive polymers; ATR-FTIR spectroscopy; Eudragit L; Eudragit S

Introduction

Gastroresistant tablets are delayed-release tablets intended to resist the gastric fluid and to release active ingredients in the intestinal lumen. Despite the simple concept on which such pH-dependent dosage forms are based, attention needs to be paid to the complexity of the GI tract and the considerable number of physiological variables, including fluid volume, fluid composition, transit, motility, bacteria and pH, which are further influenced by food, gender and age.[1]

Several studies have been conducted to identify ionic luminal fluid components that influence dissolution of coated tablets in media resembling intestinal fluid. The importance of defining ionic composition, namely buffer systems, and ionic strength of dissolution medium when determining the drug release profile was highlighted.[2] Nevertheless, other variables, such as the assumption of metal ions, such as zinc, selenium, manganese, chromium and so on, could also have

* To whom correspondence should be sent. Mailing address: Department of Pharmaceutical Sciences "Pietro Pratesi", Università degli Studi di Milano, Via L. Mangiagalli, 25, 20133, Milan, Italy. Phone: +39 02 50319349. Fax: +39 02 50319357. E-mail: giulio.vistoli@unimi.it.

(1) McConnell, E. L.; Fadda, H. M.; Basit, A. W. Gut instincts: Explorations in intestinal physiology and drug delivery. *Int. J. Pharm.* **2008**, *364*, 213–226.

(2) Fadda, H. M.; Basit, A. W. Dissolution of pH responsive formulations in media resembling intestinal fluids: bicarbonate versus phosphate buffers. *J. Drug Delivery Sci. Technol.* **2005**, *15* (4), 273–279.

10.1021/mp900199a
Published on Web 01/07/2010

an impact on the dissolution of pH-responsive polymers and, consequently, the disintegration time of coated tablets.

Among the most commonly used pH-dependent coating polymers, poly(methacrylic acid-methyl methacrylate)s (HPMMs) are weak acids which ionize and form salts in neutral conditions. Evidence reported the formation of physical cross-linking in the presence of bivalent cations, which modified swelling ability and dissolution rate of the dissociated form of these materials.[3]

Recent studies have investigated the complexation of metal ions with acidic polymers both in the gas phase and with a continuum solvatation model through density functional calculations. The obtained results are in good agreement with the experimental data, suggesting that it is possible to accurately simulate the interaction between cations and polymers by ab initio approaches.[4,5]

Despite the widespread use of HPMMs in pharmaceutics, such polymers have been rarely studied by computational approaches, and, in particular, their interactions with bications commonly present in biorelevant medium and luminal fluids have been never investigated in silico.

This work was conducted to elucidate the possible interactions and their extent among the dissociated forms of HPMMs (PMMs) and bivalent metal ions, and evaluate their impact on the solubility of PMMs and, consequently, the in vitro disintegration time and drug dissolution profile of acetaminophen gastroresistant tablets when exposed to media containing such salts.

As detailed in the Experimental Section, two types of HPMMs differing in the ratio of the monomers (namely, methacrylate and methyl methacrylate) were considered. The study of the PMM/metal ion interactions can be subdivided in two main parts. The former examined the complexes by ab initio and semiempirical calculations in the gas phase to evaluate their interactions with metal ions, while the latter analyzed experimentally the complexes by means of ATR-FTIR spectroscopy. Afterward, the results obtained by both computational and experimental analyses were confirmed by investigating the effects of such metal ions on tablet disintegration and dissolution.

Experimental Section

Materials. As depicted in Figure 1, the two considered types of HPMMs differ in the ratio of the monomers (namely, methacrylate and methyl methacrylate) which form the repeating unit. In the former ($HPMM_1$) the monomer ratio is 1:1 (Eudragit L), while in the latter ($HPMM_2$) it is equal to 1:2 (Eudragit S). Poly(sodium methacrylate, methyl methacrylate) (PMM_1, molecular weight 135,000 Da) and poly(sodium methacrylate, methylmethacrylate) (PMM_2, molecular weight 135,000 Da) were prepared as previously described.[6] Briefly, PMMs were obtained by adding NaOH pellets to 15% w/w Eudragit S100 and Eudragit L100 (Rofarma, Italy) aqueous suspension until complete salification.[6] The final solution (pH 7.1) was dried by freeze-drying (freeze-drying system Alpha 1, Martin Christ, Germany). Calcium chloride bihydrate, manganese chloride and zinc chloride were purchased by Farmalabor (Italy).

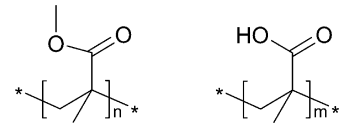

Figure 1. Structure of the modeled oligomers.

Computational Methods. *Oligomer Setup.* In the computational studies, the polymers were modeled considering representative oligomers chosen balancing reliability of simulated systems with amount of computational time. For each polymer (as depicted in Figure 1), the calculations involved the single repeating unit, and the oligomers composed of two and four repeating units (termed $1PMM_1$/$1PMM_2$, $2PMM_1$/$2PMM_2$ and $4PMM_1$/$4PMM_2$, respectively). The considered oligomers were built by VEGA[7] in their fully ionized form. To account for the stereochemical effects of such oligomers, which include two chiral centers in both repeating units, two corresponding isomers (i.e., *RR* and *RS*) were considered, while in the oligomers composed of 2 and 4 repeating units we assumed that they conserved the same configuration in the units to reduce the number of simulated molecules. After a preliminary minimization, the geometry and atomic charges were optimized by MOPAC2009. Their conformational profile was explored by a Monte Carlo procedure (as implemented in VEGA) which generated 1000 conformers by randomly rotating the rotors. All geometries so obtained were optimized and clustered according to similarity to discard redundant ones; in detail, two geometries were considered as nonredundant if they differed by more than 60 degrees in at least one torsion angle.

Molecular Dynamics. With a view to analyzing the conformational properties of such oligomers, molecular dynamics (MD) simulations were carried out in explicit water solvents. For each simulated derivative, the lowest energy conformation (as derived by previous Monte Carlo analyses) was solvated by a 15 Å thickness layer of water molecules as described by TIP3S model, and the hydrated systems were

(3) Cilurzo, F.; Selmin, F.; Minghetti, P.; Montanari, L. The effects of bivalent inorganic salts on the mucoadhesive performance of a polymethylmethacrylate sodium salt. *Int. J. Pharm.* **2005**, *301*, 62–70.

(4) Pesonen, H.; Sillanpaa, A.; Aksela, R.; Laasonen, K. Density functional study of metal ions with poly(carboxylic acid) ligands. Part 1. Poly(acrylic acid) and poly(α-hydroxy acrylic acid). *Polymer* **2005**, *46*, 12641–12652.

(5) Pesonen, H.; Sillanpaa, A.; Aksela, R.; Laasonen, K. Density functional study of metal ions with poly(carboxylic acid) ligands. Part 2. Poly(acrylic acid-co-maleic acid) poly(methyl vinyl ether-co-maleic acid), and poly(epoxy succinic acid). *Polymer* **2005**, *46*, 12653–12661.

(6) Cilurzo, F.; Minghetti, P.; Selmin, F.; Casiraghi, A.; Montanari, L. Polymethacrylate salts as new low-swellable mucoadhesive materials. *J. Controlled Release* **2003**, *88*, 43–53.

(7) Pedretti, A.; Villa, L.; Vistoli, G. VEGA: a versatile program to convert, handle and visualize molecular structure on windows-based PCs. *J. Mol. Graphics* **2002**, *21*, 47–49.

minimized to optimize the relative position of solvent molecules and to discard high-energy intramolecular interactions. The systems so obtained underwent a 5 ns MD simulation with the following characteristics: (a) spherical boundary conditions were introduced to stabilize the simulation space; (b) Newton's equation was integrated using Verlet's algorithm every 1 fs; (c) the temperature was maintained at 300 ± 10 K by means of Langevin's algorithm; (d) Lennard-Jones (L-J) interactions were calculated with a cutoff of 12 Å and the pair list was updated every 20 iterations; (e) a frame was stored every 5 ps, yielding 1000 frames; (f) no constraints were applied to the systems. The simulations were carried out in two phases: an initial period of heating from 0 to 300 K over 6000 iterations (6 ps, i.e. 1 K/20 iterations), and the monitored phase of simulation of 5 ns. Only those frames memorized during this last phase were considered. The mentioned minimizations were performed using the conjugate algorithm until an rms equal to 0.01. All calculations were carried out by Namd2.6 using the CHARMM force field.[8]

Ab Initio and Semiempirical Calculations. In order to evaluate the interaction energy of modeled oligomers with cations (i.e., Ca^{2+}, Mn^{2+} and Zn^{2+}), a combined approach was exploited. Indeed, the complexes of considered cations with the simplest $1PMM_1/1PMM_2$ oligomers were analyzed by both DFT ab initio and semiempirical calculations to assess the capacity of the latter to conveniently evaluate the interaction energies. Then, since the energies provided by semiempirical approach are in line with those computed by ab initio method, the complexes of larger oligomers ($2PMM_1/2PMM_2$ and $4PMM_1/4PMM_2$) were investigated by semiempirical approaches only. The complexes with metal ions (i.e., Ca^{2+}, Mn^{2+} and Zn^{2+}) were built starting from the lowest energy geometry of the oligomers as derived by Monte Carlo simulations. In general, we began with Zn^{2+} complexes, and then used the optimized geometry of such complexes as a starting geometry for other metals.

The quantum chemical calculations were carried out by the GAMESS program at the Becke3−Lee−Yang−Parr (B3LYP) level of theory with standard 6-31G* basis set.[9] The optimized geometry corresponding to the minimum on the potential energy surface has been obtained by solving self-consistent field equation iteratively. For Ca^{2+} and Zn^{2+} complexes, the spin restricted formalism was employed, while the Mn^{2+} complexes were taken to be in the high spin state.

The semiempirical calculations were carried out by MOPAC2009, as implemented in the VEGA program, using the PM6 level which is based on the neglect of diatomic differential overlap (NDDO) calculations and affords truly reliable results becoming a valid alternative method for predicting electronic properties of extended systems, for which ab initio methods were still prohibitive. In all cases, the ionic interactions (ΔE_{int}) were evaluated as energy difference between the complex and the two interaction partners alone ($\Delta E_{int} = E_{complex} - (E_{polymer} + E_{ion})$).

ATR-FTIR Spectroscopy. The interactions between the two types of poly(sodium methacrylate, methylmethacrylate) and the selected inorganic salts were investigated by means of ATR-FTIR spectroscopy (Spectrum One, Perkin-Elmer Italia, Italy).

Sample Preparation. A 4% w/w aqueous solution of PMM_1 or PMM_2 was prepared and stored at 25 °C for 24 h. Afterward, a 10% w/v aqueous solution of $CaCl_2$, $MnCl_2$ or $ZnCl_2$ was added and the obtained slurries were gently stirred for 30 min. After 24 h of rest, the mixtures were freeze-dried (freeze-drying system Alpha 1, Martin Christ, Germany). The ratio between the polymeric dispersion and the salt solution was fixed in order to obtain a sodium methacrylate/bication molar ratio of 20/1 and 4/1. The freeze-dried mixtures were used as such or after levigation with water (powder/water ratio 1/2 or 1/3 w/w) in a mortar for 10 min.

ATR-FTIR spectra of the dried or hydrated samples were collected with 32 scans at a resolution of 4 cm^{-1} over the wavenumber region 4000−650 cm^{-1}. All measurements were performed at ambient temperature.

Tablet Preparation. A 500 g mixture of acetominophen DC (25% w/w), Avicel PH102 (75% w/w), talc (4.0% w/w), colloidal silica (0.5% w/w) and magnesium stearate (0.5% w/w) was tableted in a rotary machine (AR 18 Ronchi, Italy) at 3000 kp equipped with concave punches (8 mm diameter).

Tablets (core weight = 199 ± 4 mg; crushing force: 60 ± 20 N) were coated in a top-spray fluid bed (Uniglatt, Glatt GmbH, Germany) equipped with a peristaltic pump (VRX 88, Verder GmbH, Germany) connected with a two-fluid atomizer through a neoprene tubing (4 mm diameter). The coating formulation consisting of an aqueous dispersion of Eudragit L 100 (11.1% w/w), triethyl citrate (5.5% w/w), 1 N NH_3 (3.7% w/w) and talc (5.5% w/w) dispersion was prepared according to the Application Technology Sheet "Enteric coating with Eudragit® L/S from aqueous dispersion" provided by the polymer manufacturer (Rohm, Germany). The coating process was performed under the following operating conditions: 390 g batch size, 58−60 °C inlet air temperature, 36−38 °C outlet air temperature, 35−40 °C product temperature, 75 inlet air flap position, 1.2 mm nozzle port size, 2.0 bar atomizing pressure, and 4.4 g/min spray rate.

Disintegration Test. Disintegration time was determined in 800 mL of 0.1 N HCl and then purified water, or $ZnCl_2$ or $CaCl_2$ aqueous solutions (0.1; 0.3; 0.6% w/v) at 37 ± 0.5 °C using a tablet disintegration test machine (Pharma Test, Germany) without disk. Before testing, the pH of the media was adjusted to pH 6.8 with 0.01 N NaOH or 0.01 N HCl. The disintegration time of 6 individual tablets was recorded.

(8) Phillips, J. C.; Braun, R.; Wang, W.; Gumbart, J.; Tajkhorshid, E.; Villa, E.; Chipot, C.; Skeel, R. D.; Kalé, L.; Schulten, K. Scalable molecular dynamics with NAMD. *J. Comput. Chem.* **2005**, *26*, 1781–802.

(9) Guest, M. F.; Bush, I. J.; van Dam, H. J. J.; Sherwood, P.; Thomas, J. M. H.; van Lenthe, J. H.; Havenith, R. W. A.; Kendrick, J. The GAMESS-UK electronic structure package: algorithms, developments and applications. *Mol. Phys.* **2005**, *103*, 719–747.

Table 1. Conformational and Physicochemical Descriptors as Derived by MD Simulations in Water[a]

oligomer	HB	PSA	MLP	SAS	ASA	dist	PSA/at	SAS/at	ASA/at	dist/at
1PMM$_1$ *RR*	26	96.09	2.04	441.60	345.51	6.25	2.83	12.99	10.16	0.18
1PMM$_1$ *RS*	23	97.66	1.99	439.33	341.67	5.72	2.87	12.92	10.05	0.17
1PMM$_2$ *RR*	24	128.11	2.39	570.52	442.41	7.21	2.78	12.40	9.62	0.16
1PMM$_2$ *RS*	20	122.26	2.37	557.27	435.01	6.92	2.66	12.11	9.46	0.15
2PMM$_1$ *RR*	49	184.17	2.22	652.70	468.54	9.45	3.07	10.88	7.81	0.16
2PMM$_1$ *RS*	43	176.58	2.24	647.61	471.03	8.44	2.94	10.79	7.85	0.14
2PMM$_2$ *RR*	50	206.35	3.45	884.69	678.34	13.02	2.37	10.17	7.80	0.15
2PMM$_2$ *RS*	49	225.61	3.28	883.17	657.57	10.40	2.59	10.15	7.56	0.12
4PMM$_1$ *RR*	68	351.96	2.53	1060.91	708.95	15.94	3.14	9.47	6.33	0.14
4PMM$_1$ *RS*	81	348.94	2.61	1055.70	706.76	9.27	3.12	9.43	6.31	0.08
4PMM$_2$ *RR*	96	420.46	5.29	1503.81	1083.35	19.78	2.49	8.90	6.41	0.12
4PMM$_2$ *RS*	115	398.60	4.75	1433.27	1034.67	15.71	2.36	8.48	6.12	0.09

[a] Concerning PSA, SAS, ASA (expressed in Å^2), and dist (expressed in Å) parameters, the table compiles also the corresponding values normalized per number of atoms.

No other salts that could interfere on the impact of the selected metal ions were added.

Dissolution Test. The dissolution test was performed using an automated apparatus SR8 Plus dissolution test station (Hanson, USA) connected to a UV spectrophotometer (DU 640 spectrophotometer, Beckman Coulter, USA). The tablets were immersed in 1000 mL of 0.1 N HCl or purified water, or $ZnCl_2$ or $CaCl_2$ aqueous solutions (0.1; 0.3; 0.6% w/v) and were stirred at 50 rpm at 37 ± 0.5 °C. Samples were withdrawn in an automated regime using a peristaltic pump and assayed for acetominophen at 241 nm. The experiments were conducted in triplicate.

Results

Computational Results. Conformational Profiles of the Oligomers. Before analyzing in silico the complexes between polymers and metal cations, the considered oligomers underwent MD simulations in water aiming to better analyze their conformational and property spaces,[10] and to unveil how the chiral centers could influence the monitored molecular properties. Hence, Table 1 compiles relevant physicochemical and geometrical descriptors as derived by MD runs. For each oligomer, Table 1 reports the mean values of the solvent accessible surface area (SAS), polar surface area (PSA) and apolar surface area (ASA) as well as the average number of H-bonds between oligomer and water molecules as computed by HBAT,[11] and the virtual log *P* mean as derived by the MLP approach.[12] Moreover, Table 1 collects also the mean distances between the two terminal methyl groups as a reliable index of the folding degree for the simulated oligomers. Since all mentioned parameters increase unavoidably with the size of the monitored oligomers, Table 1 includes also the average values normalized per the number of atoms to highlight intrinsic profiles of such descriptors.

A bird's eye analysis of Table 1 unveils that the mean values of the monitored distances and the corresponding normalized values showed contrasting trends. Indeed, the mean distances clearly increased with the size of the oligomers, while the normalized values tended to decrease from small oligomers (with one repeating unit) to larger oligomers (with two and four repeating units). This means that the oligomers assumed gradually more folded conformations increasing their molecular size. Such a trend may suggest that the electrostatic repulsions overcame the apolar contacts for small oligomers, while the hydrophobic interactions assumed a relevant role and favored more folded geometries for large oligomers. The key role of apolar contacts in the PMM polymers was confirmed by their macromolecular structure, which can show multiple-stranded complementary helices, largely stabilized by van der Waals interactions.[13] Such a conformational trend reflected on normalized means of surface values (i.e., polar surface, apolar surface and total surface), since normalized polar surface means were quite constant irrespective of the oligomer length, while normalized apolar surface values and, consequently, normalized total surface values gradually decreased when increasing the oligomer size. Even avoiding a systematic description of all rotatable torsions for the considered oligomers, a deeper analysis of MD simulations unveiled that the rotatable bonds of the 1PMM derivatives preferentially assumed antiperiplanar conformations, which induced more extended structures, while the abundance of synclinal conformations increased in the larger oligomers especially in the central monomers inducing more folded geometries. The conformational profile appears also influenced by chiral centers since the oligomers containing the like stereoisomer (i.e., *RR*) approached the polar moieties and assumed more

(10) Vistoli, G.; Pedretti, A.; Testa, B. Assessing drug-likeness—What are we missing? *Drug Discovery Today* **2008**, *13*, 285–294.

(11) Tiwari, A.; Panigrahi, S. K. HBAT: a complete package for analysing strong and weak hydrogen bonds in macromolecular crystal structures. *In Silico Biol.* **2007**, *7*, 651–61.

(12) Gaillard, P.; Carrupt, P. A.; Testa, B.; Boudon, A. Molecular lipophilicity potential, a tool in 3D-QSAR. Method and applications. *J. Comput.-Aided Mol. Des.* **1994**, *8*, 83–96.

(13) Kumaki, J.; Kawauchi, T.; Ute, K.; Kitayama, T.; Yashima, E. Molecular weight recognition in the multiple-stranded helix of a synthetic polymer without specific monomer-monomer interaction. *J. Am. Chem. Soc.* **2008**, *130*, 6373–80.

Table 2. Interaction Energies (ΔE_{int} Expressed in kJ/mol) as Derived by DFT Calculations for Simplest Oligomers

oligomer	Zn^{2+}	Mn^{2+}	Ca^{2+}
$1PMM_1$ *RR*	−2088.1876	−1798.2673	−1490.6771
$1PMM_1$ *RS*	−2146.2435	−1853.2547	−1533.7353
$1PMM_1$ mean	−2110.7464	−1825.76	−1512.21
$1PMM_2$ *RR*	−2178.1828	−1852.3474	−1553.3278
$1PMM_2$ *RS*	−2230.1618	−1917.3444	−1681.7202
$1PMM_2$ mean	−2204.1723	−1884.85	−1617.52

extended conformations to minimize the electrostatic repulsion, whereas the derivatives with the unlike stereoisomer (i.e., *RS*) arranged the polar groups in opposite directions assuming more folded geometries. Such a behavior, which was also detectable in the physicochemical properties in Table 1, was clearly visible in 1PMMs and, to a minor extent, 2PMMs, while the hydrophobic collapse rendered the conformation profile of 4PPMs less influenced by the stereochemistry.

Finally, a correlative analysis between the molecular properties as compiled in Table 1 unveiled some interesting correlations. Such relationships were focused on the normalized means because the correlations between property averages could be artifactually enhanced by the oligomer size. Thus, eq 1 reports the remarkable correlation between normalized virtual log *P* means and normalized means of both polar and apolar surfaces. Clearly, the apolar surface increased the log *P* value while the polar surface has an opposite effect as denoted by the negative sign.

$$\log P\,(\mathrm{MLP})_{\mathrm{Norm}} = 8.46 \times 10^{-3}\,\mathrm{ASA}_{\mathrm{Norm}} - 7.03 \times 10^{-3}\,\mathrm{PSA}_{\mathrm{Norm}} - 7.49 \times 10^{-3}$$
$$n = 12;\ r^2 = 0.98;\ s = 0.001735;\ F = 585.90 \qquad (1)$$

This relationship emphasizes the known role of both polar and apolar surfaces in determining the lipophilicity of a given molecule and appeared as a convincing validation of both performed simulations and algorithms used to compute such molecular properties. Taken globally, the MD simulations shed light on some important conformational properties of such oligomers and underlined significant differences among the simulated stereoisomers. This suggests that the stereochemistry could also influence the strength of metal complexes and, thereby, justified that the following computations were carried out considering the two monitored stereoisomers for each set of oligomers.

DFT Evaluation of Simplest Metal Complexes. For the simplest oligomers (1PMMs), the electrostatic interactions with three metal ions characterized by an increasing electronegativity (namely, Ca^{2+}, Mn^{2+}, and Zn^{2+}) were evaluated through DFT calculations. The DFT calculations were carried out in the gas phase considering the ionized forms of 1PMMs with one metal ion (complex's charge: +1).

Table 2 compiles the interaction energy values (ΔE_{int} expressed as kJ/mol) for the described sets of DFT calculations. For an easy comparison, Table 2 reports also the mean values for each pair of isomers. In all monitored cases, the energy values were in line with the metal electronegativity (i.e., $Zn^{2+} < Mn^{2+} < Ca^{2+}$) and in encouraging agreement with both experimental and calculated values already reported in literature.[4,5] Unlike enantiomers yielded lower energies than like enantiomers probably because in the former the ester groups can better approach the cation, while $1PMM_2$ oligomers elicited stronger interactions clearly due to the presence of two ester groups.

Even if a detailed conformational analysis of the obtained complexes goes beyond the objectives of the study, Figure 2 depicts the minimized complexes for the two isomers of $1PMM_1$ with Zn^{2+} ion. Evidently, in both isomers the two polar functions (carboxylate and ester) are turned toward the metal ion irrespective of the conformational profile as seen in water simulations and described before. Nonetheless, there was a significant difference between the two complexes. Indeed, in the *RR* enantiomer the ester group interacts with the Zn^{2+} ion through its oxygen atom, whereas in the *RS* enantiomer the ester group interacts approaching its carbonyl's oxygen atom. This difference reflects on the arrangement of metal ion in respect to oxygen atoms. As depicted in Figure 2, the three involved oxygen atoms of the *RR* isomer were almost equally distant from the Zn^{2+} ion, whereas the three interacting oxygens of the *RS* isomer showed significant differences in their distances with the metal ion. Particularly, such diversities concerned the carboxyl oxygen atoms which asymmetrically interacted with the metal ion since there was a difference of about 0.1 Å between their distances.

Semiempirical Evaluation of Larger Metal Complexes. As described in the Experimental Section, the largest oligomers (2PMMs and 4PMMs) were analyzed only by semiempirical methods, while the simplest ones (1PMMs) were evaluated by both ab initio and semiempirical approaches (as compiled in Table 3) with a view to assessing whether energy values produced by semiempirical methods were in satisfactory agreement with those by DFT calculations. Figure 3 reports the remarkable correlation between these two sets of energy values as obtained for 1PMM oligomers. Although the values obtained by the PM6 level were different from the DFT results, Figure 3 demonstrates that the semiempirical energies were in clear agreement with those provided by ab initio methods and, indeed, in all sets of PM6 calculations, the electronegativity trend (i.e., $Zn^{2+} < Mn^{2+} < Ca^{2+}$) was suitably fulfilled. Although the metal interaction energy is computationally very delicate, the results obtained for the simplest complexes confirm the reliability of PM6 level to investigate metal complexes and suggested that such a semiempirical approach could be exploited to analyze large complexes for which DFT methods were nearly unfeasible.

Specifically, four sets of semiempirical calculations were then realized: (i) fully deprotonated forms of 2PMMs with one metal ion (complex's charge: 0); (ii) monodeprotonated forms of 2PMMs with one metal ion (complex's charge: +1); (iii) fully deprotonated forms of 4PMMs with one metal ion (complex's charge: +2); (iv) bideprotonated forms of

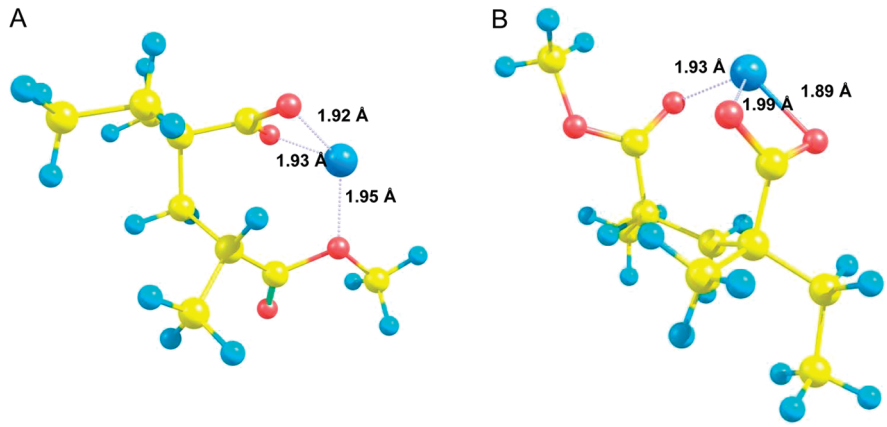

Figure 2. The minimized complexes for the (a) 1PMM$_1$ *RR* and (b) 1PMM$_1$ *RS* with Zn^{2+} ion. The figure also displays the distance between metal and interacting oxygen atoms.

Table 3. Interaction Energies (ΔE_{int} Expressed in kJ/mol) as Derived by Semiempirical PM6 Calculations for All Simulated Oligomers

oligomer	Zn^{2+}	Mn^{2+}	Ca^{2+}
1PMM$_1$ *RR*	−1398.96	−1289.98	−1273.31
1PMM$_1$ *RS*	−1429.09	−1342.75	−1305.92
1PMM$_1$ mean	−1414.03	−1316.37	−1289.62
1PMM$_2$ *RR*	−1504.72	−1361.89	−1291.19
1PMM$_2$ *RS*	−1504.53	−1334.7	−1318.59
1PMM$_2$ mean	−1504.63	−1348.3	−1304.89
2PMM$_1$ *RR*	−2291.16	−2094.02	−2013.73
2PMM$_1$ *RS*	−2349.43	−2168.41	−2055.18
2PMM$_2$ mean	−2320.3	−2131.22	−2034.46
2PMM$_2$ *RR*	−2322.04	−2121.86	−2022.5
2PMM$_2$ *RS*	−2368.35	−2172.74	−2113.87
2PMM$_1$ mean	−2345.2	−2147.3	−2068.19
2PMM$_1$_H *RR*	−1462.28	−1342.02	−1327.71
2PMM$_1$_H *RS*	−1538.89	−1425.41	−1392.08
2PMM$_1$_H mean	−1500.59	−1383.72	−1359.9
2PMM$_2$_H *RR*	−1478.73	−1389.01	−1339.97
2PMM$_2$_H *RS*	−1514.35	−1460.78	−1369.74
2PMM$_2$_H mean	−1496.54	−1424.9	−1354.86
4PMM$_1$ *RR*	−3300.31	−2922.24	−2853.73
4PMM$_1$ *RS*	−2934.56	−2663.09	−2553.25
4PMM$_1$ mean	−3117.44	−2792.67	−2703.49
4PMM$_2$ *RR*	−3479.54	−3048.63	−2994.98
4PMM$_2$ *RS*	−2994.58	−2833.02	−2490.47
4PMM$_2$ mean	−3237.06	−2940.83	−2742.73
4PMM$_1$_H2 *RR*	−2449.36	−2323.1	−2220.66
4PMM$_1$_H2 *RS*	−2089.07	−1876.07	−1786.01
4PMM$_1$H2 mean	−2269.22	−1999.59	−2003.33
4PMM$_2$_H2 *RR*	−2293.74	−2008.98	−1973.33
4PMM$_2$_H2 *RS*	−2288.7	−2115.04	−1743.46
4PMM$_2$_H2 mean	−2291.22	−2062.01	−1858.39

4PMMs with one metal ion (complex's charge: 0). The partially deprotonated species were considered since it is known that the acidic polymers with high charge density show a sharp increase of their pK_a value with α about equal to 0.5.[14] This interesting property may be related to intramolecular hydrogen bonding between the dissociated and undissociated carboxyl acid groups. All sets of oligomers

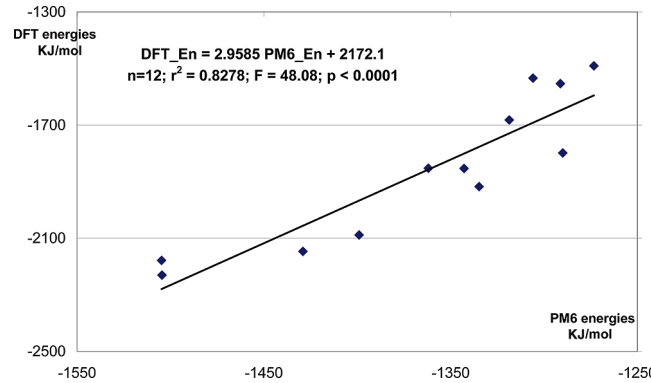

Figure 3. Remarkable correlations between interaction energy values obtained by DFT ab initio and PM6 semiempirical calculations.

were performed considering two possible configurations for the repeating unit (i.e., *RR* and *RS*).

Table 3 collects the so obtained interaction energies allowing some relevant observations. First, in all sets of PM6 calculations for such larger oligomers the already observed trend (i.e., $Zn^{2+} < Mn^{2+} < Ca^{2+}$) was suitably fulfilled suggesting that the strength of metal−oligomer interaction mainly depended on metal electronegativity irrespective of oligomer complexity. Second, the interaction energy increased with the number of carboxylates involved in the ion pairs and this trend was well recognizable considering that monodeprotonated 2PMMs showed interaction energies very similar to the corresponding 1PMMs and, similarly, bideprotonated 4PMMs had energy values comparable to the corresponding 2PMMs. Again, the effect of polar groups was observable considering that PMM$_2$s always showed better energy values than PMM$_1$s. Noticeably, there was a truly linear correlation between the energy values for the considered metal ions (e.g., ΔE_{Zn} vs ΔE_{Mn}, $r^2 = 0.994$, $n = 20$) suggesting that the interaction capacities of such representative oligomers did not depend on interacting metal. Finally, the influence of stereochemistry on interaction energy as seen

(14) Kawaguchi, S.; Kitano, T.; Ito, K.; Minakata, A. Dissociation behavior of poly(fumaric acid) and poly(maleic acid). II. Model calculation. *Macromolecules* **1990**, *23*, 731–738.

Table 4. Interaction Energies (ΔE_{int} Expressed in KJ/mol) as Derived by Semiempirical PM6 Calculations for Cross-Linked Complexes of the 2PMM Oligomers

oligomer	Zn^{2+}	Mn^{2+}	Ca^{2+}
$2PMM_1$ *RR*	−2591.86	−2507.32	−2097.52
$2PMM_1$ *RS*	−2485.49	−2405.73	−1933.18
$2PMM_1$ mean	−2538.68	−2456.53	−2015.35
$2PMM_2$ *RR*	−2719.67	−2677.45	−2198.78
$2PMM_2$ *RS*	−2655.39	−2597.49	−2149.71
$2PMM_2$ mean	−2687.53	−2637.47	−2174.25

in the simplest 1PMMs (i.e., *RS* < *RR*) is still observed in 2PMMs but vanishes in 4PMMs probably as the effects of chiral centers fade into the oligomer complexity.

A bird's eye analysis of the conformation for the simulated complexes shows that 2PMMs conserved a quite extended geometry as derived by MD simulations, whereas 4PMMs assumed more folded structures curled around the metal ion. Although the 4PMM energies were in line with the expected trend, such a folded conformation appeared quite unphysical also considering that these representative oligomers were in fact embedded in large polymers being characterized by well-defined folding which should not undergo such a structural collapse. Overall, the reported simulations suggested that the most promising compromise between computational reliability and oligomer complexity (and consequently computational effort) is represented by 2PMMs molecules. Indeed, although all considered oligomers show interaction energies in line with the metal electronegativity, only 2PMMs conserved a quite extended conformation and were still influenced by chiral centers.

Hence, 2PMMs were exploited to investigate the cross-linking effects by simulating suitable complexes made by two 2PMM oligomers interacting with a central metal ion. Table 4 compiles the interaction energies as obtained for such complexes and unveils a distribution of energy values markedly different compared to that derived for complexes with only one oligomer. Indeed, Table 3 reports homogeneously distributed energy values (as assessed by aforementioned linear relations) in which the energy for Mn^{2+} was exactly placed in between the values for Zn^{2+} and Ca^{2+} which represent the limits of such trends. Conversely, Table 4 shows that Zn^{2+} and Mn^{2+} cross-linked complexes showed very similar energy values being largely lower than that for Ca^{2+} complex even if Zn^{2+} complexes had always the lowest interaction energies. In other words, the electronegativity trend was fulfilled also by cross-linked complexes, but the distribution of these energies was markedly different allowing the recognition of two clusters since Zn^{2+} and Mn^{2+} cross-linked complexes appeared vastly more stable than Ca^{2+} complexes. These different features are consistent with the precipitation of PMMs from 4% w/v solutions when $MnCl_2$ and Zn Cl_2 were added.

A visual scrutiny of the optimized cross-linked complexes can explain their different behavior. Indeed the complexes with Zn^{2+} and Mn^{2+} ions showed a similar and slightly bent

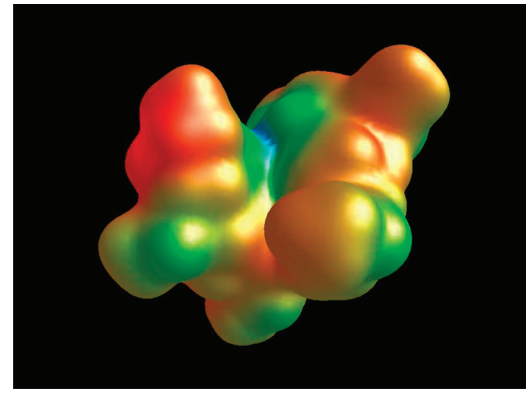

Figure 4. MLP surface for the complex built by two $2PMM_1$ *RR* oligomers (blue polar zone and red hydrophobic areas).

conformation of the oligomers which appeared fittingly arranged so to bury the ion pairs inside the complex maximizing the hydrophobic interactions between oligomers. Conversely, the Ca^{2+} cross-linked complexes assumed a more extended structure which cannot entirely shield the ion pairs and reduced the complementarities of apolar interactions as seen in the other complexes. The key role of hydrophobic contacts was shown by MLP surface for $2PMM_1$ *RR*−Zn^{2+} cross-linked complexes as depicted by Figure 4. It is worth noting that the displayed surface is almost totally apolar (red/yellow areas) and the polar areas (blue) are confined in the center of the complex, a zone which should be fully inaccessible when considering larger polymers.

ATR-FTIR Spectroscopy. The carboxylate (COO^-) groups can coordinate to metal ions in a number of modes: "monodentate" (or "unidentate"), "bidentate" (or "chelating"), "bridging" (or "bridging bidentate") modes.[15,16] When a metal ion interacts with only one oxygen atom of a COO^- group, the coordination structure is regarded as monodendate. In the bidentate coordination mode, the metal ion interacts equally with the two oxygen atoms of a COO^- group. In the bridging coordination mode, one metal ion binds to one of the two oxygen atoms in a COO^- group and another metal ion to the other oxygen atom. Deacon and Phillips[9] found a general tendency in the relationship between $\Delta\nu_{a-s}$ (frequency separation between the COO^- antisymmetric and symmetric stretching vibrations) and the coordination type of the COO^- group to metal ions by examining the structures and vibrational frequencies of a number of acetate salts in the solid state. Due to the decrease in equivalence of the C−O bonds, the frequency of the COO^- antisymmetric stretch of the unidentate species is higher than that of the ionic (metal-free) species, which is in turn higher than that of the bidentate species. The reverse is the case for the COO^-

(15) Deacon, G. B.; Phillips, R. J. Relationships between the carbon-oxygen stretching frequencies of carboxylate complexes and the type of carboxylate coordination. *Coord. Chem. Rev.* **1980**, *33*, 227–250.

(16) Nakamoto, K. *Infrared and Raman Spectra of Inorganic and Coordination Compounds Part B*, 5th ed.; Wiley: New York, 1997, pp 57−62.

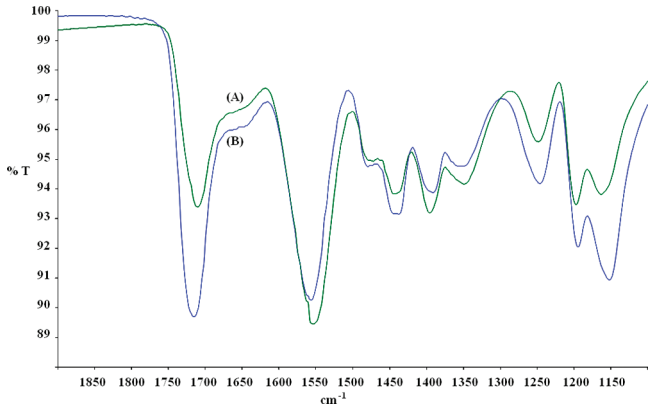

Figure 5. ATR-FTIR spectra of dried (A) PMM_1 and (B) PMM_2.

Table 5. Shift of $\nu_{as}(COO^-)$ and $\nu_s(COO^-)$ Bands of PMM_1 and PMM_2 in the Presence of the Inorganic Salts at the Molar Ratio 4/1[a]

		dried			hydrated		
copolymer	salt	$\nu_{as}(COO^-)$	$\nu_s(COO^-)$	$\Delta\nu$	$\nu_{as}(COO^-)$	$\nu_s(COO^-)$	$\Delta\nu$
PMM_1		1553	1349	204	1543	1346	197
	$CaCl_2$	1548	1360	188	1544	1357	187
	$MnCl_2$	1542	1359	183	1539	1352	187
	$ZnCl_2$	1574	1346	228	1557	1349	208
PMM_2		1556	1353	203	1548	1349	199
	$CaCl_2$	1556	1360	196	1548	1361	187
	$MnCl_2$	1556	1360	196	1542	1354	188
	$ZnCl_2$	1568	1358	210	1575	1350	225

[a] All values are expressed in cm^{-1}.

symmetric stretch. As a result, the $\Delta\nu_{a-s}$ values for monodentate, bridging, bidentate and ionic species are in the following order:

$$\Delta\nu_{a-s}(\text{unidentate}) > \Delta\nu_{a-s}(\text{ionic}) \sim \Delta\nu_{a-s}(\text{bridging}) > \Delta\nu_{a-s}(\text{bidentate})$$

The empirical rule described above can be applied to other compounds, such as proteins containing aminocarboxylate groups, although the value $\Delta\nu_{a-s}$(ionic) depends on the considered compound.[15–17]

Fourier-transform infrared spectroscopy (FTIR) is a useful tool for investigating metal ion−carboxylate coordination in different environment. As previously described,[6] the main differences in the spectra of dry PMMs reside in the relative intensities of bands attributed to the C═O stretching vibration of the esteric group at about 1710 cm^{-1}, $\nu_a(COO^-)$ and $\nu_s(COO^-)$ at about 1550 and 1350 cm^{-1} and about 1560 and 1350 cm^{-1} for PMM_1 and PMM_2 respectively, which reflect the different content of the monomers in the two copolymer chains (Figure 5). The value of $\Delta\nu_{a-s}$(ionic) of both PMMs was up to 200 cm^{-1} (Table 5).

At the water/PMM ratio of 1/2 w/w, the band at 1645 cm^{-1} assigned to the symmetric stretch of the water molecules was clearly detectable and $\nu_a(COO^-)$ and $\nu_s(COO^-)$ and C═O ester groups shifted toward lower wavenumbers for both copolymers (Table 5). The shift of $\nu_a(COO^-)$ was more significant than that of $\nu_s(COO^-)$ and, consequently, the $\Delta\nu_{a-s}$(ionic) of both PMMs decreased to values lower than 200 cm^{-1}. These modifications were attributed to the formation of H-bond interactions between these functional groups and water.[3] As expected, when the water content was increased, only the intensity of the mid-infrared bands of water at 3500−2500 cm^{-1} and 1645 cm^{-1} increased (data not shown).

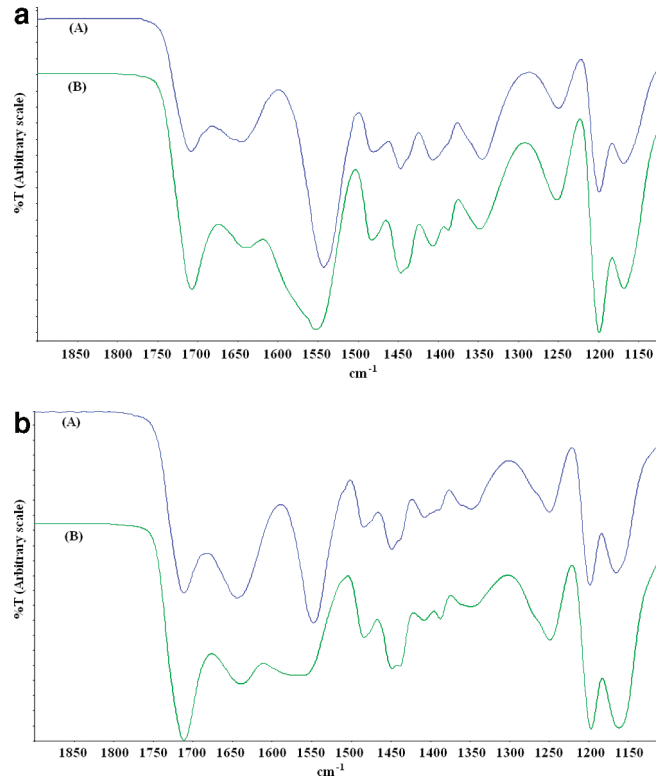

Figure 6. (a) ATR-FTIR spectra of (A) hydrated PMM_1 and (B) $PMM_1/ZnCl_2$ blend at the 4/1 ratio. (b) ATR-FTIR spectra of (A) hydrated PMM_2 and (B) $PMM_2/ZnCl_2$ blend at the 4/1 ratio.

The spectra recorded on the dry or hydrated metal ion/PMM blends at the 1/20 molar ratio did not show any significant shift of the most relevant bands. Increasing the Mn^{2+} or Ca^{2+}/PMM molar ratio to 1/4, the value of $\Delta\nu_{a-s}$ decreased by at least 7 cm^{-1} (Table 5), indicating that the COO^- group bound both cations in the bidentate coordination mode. On the contrary, the addition of Zn^{2+} to both PMMs determined the increase of $\Delta\nu_{a-s}$ values, suggesting that the COO^- groups coordinated the metal ion in monodentate coordination mode. The hydration of the blends did not cause a variation of the coordination mode.

The ionic interactions between the metal ions and the COO^- groups of PMMs were also supported by morphologic changing of the shape of $\nu_a(COO^-)$. The greater the electronegativity of the cation, the broader the band shape and the weaker the band intensity. This phenomenon was clearly remarkable in the case of Zn^{2+} (Figure 6). The

(17) Dudev, T.; Lim, C. Monodentate versus bidentate carboxylate binding in magnesium and calcium proteins: what are the basic principle? *J. Phys. Chem. B* **2004**, *108*, 4546–4557.

Table 6. Heights of the $\nu_{as}(COO^-)$ and stretching vibrations of C═O ester bands and their ratio

			dried			hydrated		
copolymer	salt	ratio	$\nu_{as}(COO^-)$	C═O	$\nu_{as}(COO^-)$/C═O ratio	$\nu_{as}(COO^-)$	C═O	$\nu_{as}(COO^-)$/C═O ratio
PMM_1			0.0521	0.0331	1.574	0.1082	0.0595	1.818
	$CaCl_2$	20/1	0.0259	0.0165	1.570	0.1025	0.0562	1.824
	$MnCl_2$	20/1	0.0193	0.0130	1.485	0.0916	0.0503	1.821
	$ZnCl_2$	20/1	0.0358	0.0246	1.455	0.0973	0.0581	1.675
	$CaCl_2$	4/1	0.0291	0.0183	1.590	0.0406	0.0244	1.664
	$MnCl_2$	4/1	0.0329	0.0269	1.223	0.0584	0.0421	1.387
	$ZnCl_2$	4/1	0.0242	0.0218	1.110	0.0685	0.0613	1.117
PMM_2			0.0313	0.0335	0.934	0.0582	0.0532	1.094
	$CaCl_2$	20/1	0.0430	0.0465	0.925	0.0608	0.0572	1.063
	$MnCl_2$	20/1	0.0463	0.0517	0.896	0.0660	0.0629	1.049
	$ZnCl_2$	20/1	0.0377	0.0435	0.867	0.0555	0.0540	1.028
	$CaCl_2$	4/1	0.0223	0.0225	0.991	0.0462	0.0454	1.018
	$MnCl_2$	4/1	0.0186	0.0256	0.727	0.0176	0.0196	0.898
	$ZnCl_2$	4/1	0.0276	0.0386	0.715	0.0415	0.0659	0.630

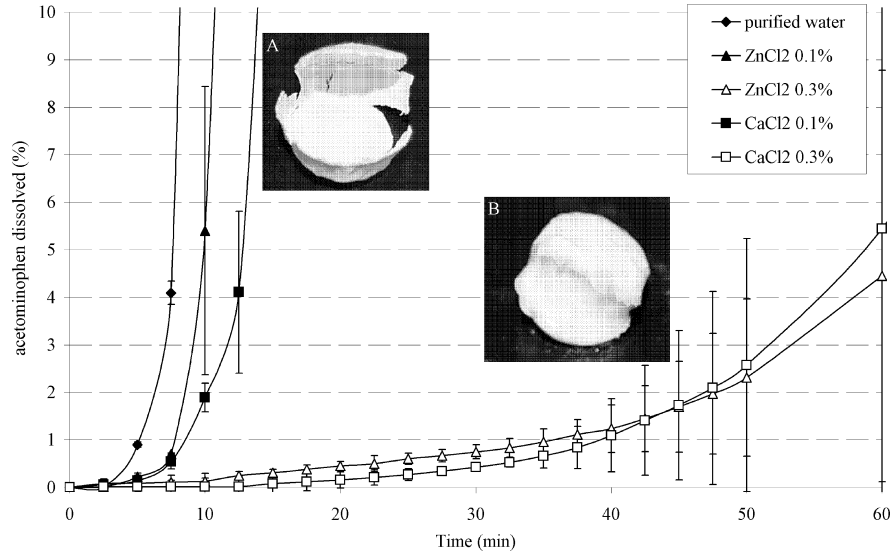

Figure 7. Dissolution profiles of acetaminophen in presence of $ZnCl_2$ or $CaCl_2$ at different concentrations. The inserts show the tablet at the end of the experiments performed in (A) 0.1% w/v and (B) 0.3% w/v $ZnCl_2$ aqueous solutions.

decrease of the $\nu_a(COO^-)$ intensity was taken as a semiquantitative indication of the interaction strength between the metal ion and the carboxylate moieties of PMMs. Indeed, as reported in Table 6, the ratio between the transmittance of the C═O stretching vibration of the ester groups and $\nu_a(COO^-)$ of both PMMs resulted strongly influenced by all considered variables, namely, the type and concentration of the metal ions and the presence of water, and indicated that the ionic interactions between polymers and cations parallel the metal electronegativity (i.e., $Zn^{2+} < Mn^{2+} < Ca^{2+}$).

Effect of Bivalent Metal Ions on Tablet Disintegration and Acetaminophen Dissolution. The coated tablets complied with the gastroresistance requirement since they were stable in acidic condition for 2 h and then disintegrated in purified water within 15 min. In the presence of Zn^{2+} and Ca^{2+}, the tablets disintegrated, but large fragments of the coating remained in the basket after 3 h, independently of the type and concentration of the metal ion. When $ZnCl_2$ solutions were used, the tablet break visually occurred after 20 min. The coating break occurred after 1 or 2.5 h when the $CaCl_2$ concentrations were set at 0.1 or 0.3% w/v, respectively. By using a 0.6% w/v $CaCl_2$ solution, the tablets remained intact over the tested period.

The dissolution profiles of acetaminophen were in agreement with the disintegration results: the higher the metal ion concentration in the dissolution medium, the more delayed the drug dissolution (Figure 7). At the highest concentration of salts, the tablets were intact at the end of the experiment.

Discussion

With a view to comparing experimental and computational results, Table 7 compiles the statistics (i.e., r^2 and F statistic) for the relationships between normalized $\nu_{as}(COO^-)$/C═O ratios and interaction energies as derived by computational analyses. Globally, the reported statistics emphasize that the experimental results are in promising agreement with the

Table 7. Statistics for the Correlations between Normalized $\nu_{as}(COO^-)/C{=}O$ Ratios and Interaction Energies as Derived by Computational Analyses (in All Equations $n = 6$)

simulated complex and used method	ratio 4/1		ratio 20/1	
	r^2	*F* statistic	r^2	*F* statistic
1PMM$_1$ *RR* DFT	0.957	88.61	0.812	17.24
1PMM$_1$ *RS* DFT	0.940	62.59	0.799	15.92
1PMM$_1$ *RR* PM6	0.828	19.23	0.730	4.02
1PMM$_1$ *RS* PM6	0.824	18.72	0.895	34.16
2PMM$_1$ *RR* PM6	0.979	182.58	0.927	50.99
2PMM$_1$ *RS* PM6	0.948	72.68	0.927	50.77
2PMM$_1$_H *RR* PM6	0.961	99.75	0.864	25.44
2PMM$_1$_H *RS* PM6	0.973	143.79	0.809	16.90
4PMM$_1$ *RR* PM6	0.849	22.55	0.831	19.66
4PMM$_1$ *RS* PM6	0.952	79.42	0.704	9.53
4PMM$_1$_H2 *RR* PM6	0.838	20.14	0.551	4.90
4PMM$_1$_H2 *RS* PM6	0.840	21.04	0.562	5.13
2PMM$_1$ *RR* cross-linked PM6	0.708	9.70	0.402	2.62
2PMM$_1$ *RS* cross-linked PM6	0.669	8.07	0.376	2.41

performed simulations and allow some interesting considerations. First, the correlations obtained by 4/1 ratio are significantly better than those obtained by 20/1 ratio (mean r^2: 0.84 vs 0.73) indicating that the increased salt concentration renders the experimental conditions more similar to the simulated complexes. Second, the relations derived using DFT calculated energies are slightly better than the corresponding equations derived by PM6 computed energies (mean r^2: 0.85 vs 0.82). This underlines the remarkable reliability of DFT derived energies but confirms that also the PM6 derived energies are precise enough to successfully predict such ionic interactions. Finally, the 2PMM oligomers afforded the best relations highlighting that these oligomers represent the best compromise between computational reliability and oligomer complexity. Conversely, the cross-linked complexes yielded the worst relations indicating that such systems are useful to rationalize the polymer precipitation rather than the specific metal complexation. From a conformational standpoint, the monodentate coordination mode as observed with Zn^{2+} ions was in agreement with the asymmetrical interaction as derived by DFT calculations for 1PMM$_1$ *RS* with Zn^{2+} ion and depicted in Figure 2b, suggesting that such a particular arrangement is the most probable irrespective of the chiral centers.

The hitherto described results clearly evidenced that the solubility of PMMs is strongly affected by bivalent metal ions. At an atomic level, the interactions between metal ions and polymers could be analyzed by ATR-FTIR spectroscopy and predicted in silico by semiempirical ionic energy values. At a macroscopic level, such effects can be evaluated by polymer precipitation due to the salt addition and can be conveniently simulated by cross-linked complexes. In order to further investigate the effect of metal ions, the tablet disintegration and acetominophen dissolution was evaluated by using Eudragit L100 that resulted more sensitive to the interactions with cations due to its higher content of carboxylic moieties.

These theoretical data justified the in vitro behavior of acetaminophen tablets. The tablet disintegration and drug dissolution were retarded by the interactions of the dissolving copolymer with the metal ions which led to coating insolubilization. The measured disintegration times were not in agreement with the electronegativity of the metal ions which is responsible for the strength of the interactions with the carboxylic moieties of PMM. Assuming that water diffuses into the tablet nuclei and cellulose microcrystalline swells determining the coating break, the different disintegration times in the presence of the two metal ions can be explained considering the different behavior of PMM/$ZnCl_2$ and PMM/$CaCl_2$ mixtures upon hydration: the latter eroded, the former swelled[3] allowing a faster water inlet.

In conclusion, even if these preliminary results should be deepened, the demonstrated interactions between metal ions and fully depronotated or partially protonated PMMs, chosen as an example of gastroresistant polymers, allow two considerations to be drawn. The former concerns the proposed in silico simulation strategy which provides seamless coupling among various oligomers and the divalent cations. The latter concerns the performances of gastroresistant dosage forms assayed in the presence of a large amount of metal ions. The anomalous behavior during the disintegration and drug dissolution tests emphasizes how the coating erosion of gastroresistant tablets could be affected by the variation of microenvironment composition. This could also occur in vivo, as an example, by the concomitant ingestion of food supplements which could dramatically increase the real concentration of inorganic salts in the intestinal milieu.

MP900199A